



An evaluation of Deccan Traps eruption rates using geochronologic data

5 Blair Schoene^{1*}, Michael P. Eddy², C. Brenhin Keller³, Kyle M. Samperton⁴,

1. Department of Geosciences, Princeton University, Princeton, NJ 08544, USA;
2. Department of Earth, Atmospheric, and Planetary Sciences, Purdue University, West Lafayette, IN 47907, USA
- 10 3. Department of Earth Sciences, Dartmouth College, Hanover, NH 03755, USA
4. Nuclear and Chemical Sciences Division, Lawrence Livermore National Laboratory, Livermore, CA 94550, USA

Correspondence to: Blair Schoene (bschoene@princeton.edu)

15

Abstract. Recent attempts to establish the eruptive history of the Deccan Traps large igneous province have used both U-Pb (Schoene et al., 2019) and ⁴⁰Ar/³⁹Ar (Sprain et al., 2019) geochronology. Both of these studies report dates with high precision and unprecedented coverage for a large igneous province, and agree that the main phase of eruptions began near the C30n-C29r magnetic reversal and waned shortly after the C29r-C29n reversal, totaling
20 the C30n-C29r magnetic reversal and waned shortly after the C29r-C29n reversal, totaling ~700-800 ka duration. Nevertheless, the eruption rates interpreted by the authors of each publication differ significantly. The U-Pb dataset was interpreted to indicate four major eruptive pulses, while the ⁴⁰Ar/³⁹Ar dataset was used to argue for an increase in eruption rates coincident with the Chicxulub impact (Renne et al., 2015; Richards et al., 2015). Although the overall
25 agreement in duration is an achievement for geochronology, the disparate eruption models may act to undermine this achievement in the eyes of the broader geologic community. Here, we generate chronostratigraphic models for both datasets using the same statistical techniques and conclude that 1) age modeling of the ⁴⁰Ar/³⁹Ar dataset results in constant eruption rates with relatively large uncertainties through the duration of the Deccan Traps, and cannot verify or
30 disprove the pulses identified by the U-Pb data, 2) the stratigraphic position of the Chicxulub impact within the ⁴⁰Ar/³⁹Ar dataset is much more uncertain than was presented in Sprain et al. (2019), and 3) neither dataset supports an increase in eruption rate as a result of the Chicxulub impact. While the production of precise and accurate geochronologic data is of course essential



to studies of Earth History, our analysis underscores that the accuracy of a final result also is
35 critically dependent on how such data are interpreted and presented to the broader community
of geoscientists.

1. Introduction

40 There is increasing recognition that volcanic activity can impact global climate on both human
and geologic timescales. This relationship is apparent from historical, explosive eruptions
(Minnis et al., 1993; Robock, 2000), and inferred for larger, effusive eruptions through the
Phanerozoic (Ernst and Youbi, 2017; Self et al., 2014). Mafic large igneous provinces (LIPs)
have been correlated with brief hyperthermal climate episodes such as the Paleocene-Eocene
45 Thermal Maximum (PETM), as well as several mass extinctions throughout the Phanerozoic
(Bond and Wignall, 2014). The reasons for such disastrous climate and ecosystem responses
remain a focus of debate among Earth historians. Critical to this discussion are precise
chronologies of LIP eruptions, particularly since they have never been observed in recorded
human history. Advances in geochronological techniques and applications over the last two
50 decades have evolved to show that LIPs erupt $>10^5$ km³, usually in less than a million years, as
opposed to tens of millions as previously thought (Kasbohm et al., in press). However, large
uncertainties remain regarding the rates of extrusive versus intrusive magmatism, as well as the
flux of volcanic volatiles, such as CO₂ and SO₂, that are thought to drive climate change (Black
and Manga, 2017; Self et al., 2014). Datasets that constrain eruption rates could be compared
55 to climate proxy records in order to understand, for example, eruptive versus non-eruptive
volatile emissions, which will lead to better models for climate and biotic system response to
LIPs.

The Deccan Traps, India, is the youngest LIP that is temporally associated with a mass
extinction, at the end of the Cretaceous Period (Fig. 1; (Courtillot et al., 1988; McLean, 1985).
60 This extinction is also famously associated with collision of the Chicxulub bolide on the southern
Mexican coast (Alvarez et al., 1980; Hildebrand et al., 1991; Smit and Hertogen, 1980), and
thus it has been debated whether or not the Deccan Traps played a role at all in the extinction
(Hull et al., 2020; Keller et al., 2008; Schulte et al., 2010). Furthermore, the temporal
coincidence of the two potentially Earth changing events has led to speculation about whether
65 the Chicxulub impactor could have had an influence on eruption rates in the Deccan Traps
(Byrnes and Karlstrom, 2018; Rampino and Caldeira, 1992; Richards et al., 2015). Impacts and



extinction aside, the Deccan Traps provide an ideal setting in which to investigate the rates of LIP volcanism within a stratigraphic context because they are relatively young and contain a well-exposed, accessible, and well-studied stratigraphy (Fig. 1; (Beane et al., 1986; Chenet et al., 2009; Chenet et al., 2008; Kale et al., 2020; Mitchell and Widdowson, 1991; Renne et al., 70 al., 2015; Schoene et al., 2015; Subbarao et al., 2000).

Two geochronological datasets appeared in the same issue of *Science* in 2019, both with the aim of establishing eruption rates of the Deccan Traps and comparing their eruption history to the climatic and biologic events associated with the mass extinction and the timing of 75 the Chicxulub impact. One paper (Sprain et al., 2019) uses $^{40}\text{Ar}/^{39}\text{Ar}$ geochronology of plagioclase from erupted basalts and the other (Schoene et al., 2019) uses U-Pb geochronology on zircon from presumed ash-bearing intervals between basalt flows. The two datasets confirm unambiguously that the main phase of eruptions began shortly before the C30n-C29r magnetic reversal and ended following the C29r-C29n magnetic reversal over a duration of ~ 700 -800 kyr, 80 corroborating published paleomagnetic data used to reach the same conclusion (Chenet et al., 2009; Chenet et al., 2008; Courtillot et al., 1986). Both studies attempted to use their respective datasets to calculate eruption rates by estimating the volume of erupted basalts as a function of time. The original plots used to illustrate the eruption rates, however, appear to show that the two geochronological datasets disagree significantly (Fig. 2). Schoene et al. (2019) use the U- 85 Pb dataset to argue that the Deccan Traps erupted in four distinct pulses separated by relative lulls in volcanism that lasted up to 100 ka or more. Sprain et al. (2019) plot the $^{40}\text{Ar}/^{39}\text{Ar}$ dataset in a way that gives the impression that there was an increase in eruption rate associated with the Chicxulub impact. Indeed, it seems that authors of subsequent papers (Henehan et al., 2019; Hull et al., 2020; Linzmeier et al., 2020; Milligan et al., 2019; Montanari and Coccioni, 90 2019), in addition to the associated News and Views piece in the same issue of *Science* (Burgess, 2019) and subsequent discussion and news coverage on *Sciencemag.org* (Kerr and Ward, 2019; Voosen, 2019), seem to conclude that the datasets do not agree on the eruption rates of the Deccan Traps.

Throughout this paper, we assume that the individual eruption ages for all samples from 95 each study are accurate as reported, and while both methods bring uncertainties to this assumption, this permits us to simply discuss how the data in each study were used to determine the eruptive history of the Deccan Traps. In doing so, we show that the conclusion is incorrect that the eruption rates derived from the datasets of Schoene et al. (2019) and Sprain et al. (2019) disagree, and that in fact they agree quite well. This confusion has arisen because



100 Fig. 4 in Sprain et al. (2019) that purports to plot eruptive flux does not have units of flux or rate
and is therefore misleading. By applying the same analysis approach to both geochronological
datasets, using correct units of volumetric eruption rate, we show that the two datasets largely
agree at their respective levels of precision, and that the lower-precision $^{40}\text{Ar}/^{39}\text{Ar}$ dataset can
neither confirm nor refute the model of pulsed eruptions established by the higher-precision U-
105 Pb dataset.

An apparent agreement in absolute ages is difficult to reconcile with systematic
uncertainties resulting from neutron fluence monitors used to calculate $^{40}\text{Ar}/^{39}\text{Ar}$ ages: adopting
a more widely used age for the Fish Canyon sanidine neutron fluence monitor shifts the
 $^{40}\text{Ar}/^{39}\text{Ar}$ dataset for the Deccan Traps and Chicxulub impact younger by about 200 ka. While
110 this does not affect the calculated duration of the Deccan Traps, the duration of the C29r
magnetic polarity chron, or the possible stratigraphic positions of the Chicxulub impact, such a
shift does undermine any apparent agreement between the $^{40}\text{Ar}/^{39}\text{Ar}$ and U-Pb datasets in
absolute time and highlights the need for continued work on intercalibration of the two
chronometers.

115

2. Correctly plotting volcanic eruption rates.

It is common to discuss volcanic flux in terms of the volume of lava erupted in a given period of
time, as cubic kilometers per year (km^3/a). We note here that we try to consistently refer to this
120 as a *rate* rather than a *flux* because units of flux include an area term that we do not know; rate
and flux are often used interchangeably in the literature, however. Either way, this calculation is
prone to large uncertainties because it requires robust estimates of eruptive volumes combined
with geochronology that is adequately precise to resolve changes in eruption rate through time.
Volume estimates for LIPs are especially difficult because they are typically deeply eroded over
125 vast areas. It is not atypical for volume estimates to vary by factors of 2-5 (Marzoli et al., 2018;
Ricci et al., 2013; Richards et al., 2015; Shellnutt et al., 2012). Furthermore, any eruptive model
is critically dependent on the regionally correlated stratigraphic architecture of the LIP, which
includes its own uncertainties. Both Schoene et al. (2019) and Sprain et al. (2019) use the same
regional stratigraphic framework and the same volume model for individual formations within the
130 Deccan Traps (Richards et al., 2015) and so while use of this model introduces significant
uncertainties in the calculated eruptive rates, these uncertainties are systematic.



The figures showing eruption rates in Schoene et al. (2019) and Sprain et al. (2019; reported as eruptive flux) appear in their Figs. 2 and 4, respectively, and are reproduced in our Fig. 2. The apparent discrepancy between the datasets is obvious, where the U-Pb dataset
135 shows four eruptive pulses and the $^{40}\text{Ar}/^{39}\text{Ar}$ appears to show a dramatic increase in eruption rate starting at the base of the Poladpur Fm. However, the box heights in Fig. 4 of Sprain et al. (2019) do not have units of flux, or rate. They correspond to the total volume of each formation [km³], rather than the eruption rate [km³/a]. As such, the apparent eruptive “flux” plotted in Fig. 4 of Sprain et al. (2019) is misleading by making it appear as if there is an increase in eruption
140 rate at the base of the Poladpur Fm. The apparent increase is because the Poladpur, Ambenali, and Mahabaleshwar are larger in the volume model of Richards et al. (2015), not necessarily because they erupted faster. We have redrafted Fig. 4 from Sprain et al. (2019) by simply dividing the volume of each formation (height of their boxes) by the estimated duration that they used for each formation (width of their boxes), to give units of volume/time (Fig. 3).
145 Note that while this is a more realistic depiction of the eruption rates derived from the $^{40}\text{Ar}/^{39}\text{Ar}$ data, this plot has difficulty taking into account the non-negligible uncertainties in formation boundary ages and therefore eruption rates.

To better compare the eruption rates that can be derived from the two datasets, we have applied the same plotting strategy from Schoene et al. (2019) to both the U-Pb and $^{40}\text{Ar}/^{39}\text{Ar}$
150 datasets. This approach assigns each sample to a position within a composite stratigraphic section plotted as cumulative volume and uses a Bayesian Markov Chain Monte Carlo (MCMC) algorithm to build an age model (Keller, 2018). Here, we use the assigned stratigraphic positions of the basalt samples from Fig. 2 of Sprain et al. (2019) and apply the same MCMC algorithm to that dataset (Fig. 4).

155 With the exception of a portion of the Ambenali Fm., the age models for the U-Pb and $^{40}\text{Ar}/^{39}\text{Ar}$ agree at the 95% credibility intervals (top panel of Fig. 4). The apparent discrepancy at the top of the Ambenali Fm. could be due to a number of reasons that are beyond of the scope of this paper, though systematic biases largely undermine the utility of comparing the absolute ages of these datasets at any particular height (see section 5 below). Eruption rates from the
160 $^{40}\text{Ar}/^{39}\text{Ar}$ dataset are relatively constant. However, the question of whether this apparent constancy provides an argument against pulsed eruptions is explored in a subsequent section. The main point here is that neither dataset shows any evidence for an increase in eruption rate associated with the Chicxulub impact (Fig. 4, and see discussion below).



165 **3. The position of the Chicxulub impact in the Deccan stratigraphy.**

The MCMC algorithm used above can also be queried to produce a probabilistic assessment of where the Chicxulub impact falls within the Deccan stratigraphy, given an age and uncertainty estimate for the impact event. Chicxulub impact dates from both U-Pb and $^{40}\text{Ar}/^{39}\text{Ar}$ methods
170 exist in the literature (Clyde et al., 2016; Renne et al., 2013; Sprain et al., 2018), allowing us to simply calculate the probability that the impact occurred at each point in our stratigraphic age model. Doing so with the U-Pb data shows that it is highly likely that the impact occurred near the top of the Poladpur Fm. (Fig. 3). The same procedure with the $^{40}\text{Ar}/^{39}\text{Ar}$ dataset shows a wider range of possible positions for the Chicxulub impact, ranging from the base of the
175 Khandala Fm. and tailing off towards the top of the Poladpur Fm. (Fig. 3). Therefore, it is unlikely that these two datasets agree as to the position of the Chicxulub impact within the Deccan Traps eruptive history.

Sprain et al. (2019) noted a similarly large uncertainty in the position of the Chicxulub impact within the Deccan Traps when evaluated using the composite stratigraphic section (Fig.
180 4). In order to avoid the uncertainty that correlation between different stratigraphic sections may impose on evaluating the position of the Chicxulub impact, they additionally approached the problem using samples that were collected from a single continuous stratigraphic section with good coverage of the upper part of the Deccan stratigraphy (the Ambenali Ghat). In their analysis, Sprain et al. (2019) subject their dataset to an available Bayesian age modeling
185 algorithm called Bacon (Blaauw and Christen, 2011). One of the premises of this algorithm is that it incorporates several assumptions about the MCMC sampling, including the requirement of priors for both accumulation/eruption rate and the memory/linearity of these rates throughout the stratigraphic sequence. The result of this approach on the dataset from Sprain et al. (2019) is that it very easily adopts a linear deposition rate, resulting in a very precise age model in
190 which the Chicxulub impact and Bushe-Poladpur contact appear coeval (Fig. 5), which forms the basis for their placing the Chicxulub impact at that formation boundary (Fig. 2).

While the merits and drawbacks of assumptions about deposition rates in sedimentary strata age modeling can be debated (and has been, e.g., (Blaauw and Christen, 2011; Haslett and Parnell, 2008; Parnell et al., 2011; Wright et al., 2017), we do not think that any
195 assumptions about eruption rate for the Deccan Traps, or any other LIP, can be justified *a priori*. So, we have instead applied our own MCMC model, which makes no assumptions about eruption rate, to the $^{40}\text{Ar}/^{39}\text{Ar}$ data from the Ambenali Ghat. The result is a much less precise



age model and also a much less certain position of the Chicxulub impact within the stratigraphy (Fig. 5). In our results, the position of the Chicxulub impact forms a probability distribution that spans as high as the middle Ambenali Fm. to well below the bottom of the section, similar to the results for the composite stratigraphic section presented in Fig. 4.

4. Testing for pulsed versus non-pulsed eruption: the importance of temporal resolution in geochronologic datasets.

We show above that neither the $^{40}\text{Ar}/^{39}\text{Ar}$ nor the U-Pb data support an increase in eruption rate in the Deccan Traps at the time of the Chicxulub impact. However, the eruption rates are distinctly different, with one model showing constant eruptions at ca. 1-2 km^3/a and the other showing pulses reaching $> 10 \text{ km}^3/\text{a}$ (Fig. 4). The average precision for each U-Pb date is ± 64 ka, whereas the average precision of the $^{40}\text{Ar}/^{39}\text{Ar}$ dates is ± 270 ka. Given the roughly factor of four to five lower analytical precision of the $^{40}\text{Ar}/^{39}\text{Ar}$ dataset compared to the U-Pb dataset, it is reasonable ask: would the $^{40}\text{Ar}/^{39}\text{Ar}$ be expected to resolve the pulses if they indeed exist in the record? There are two limiting factors that need to be considered in answering this question: 1) the stratigraphic separation between samples (i.e., pulses that aren't sampled cannot be resolved) and 2) analytical resolution (i.e., pulses that are much shorter than the analytical precision cannot be resolved). Both the U-Pb and $^{40}\text{Ar}/^{39}\text{Ar}$ datasets reported 20-30 samples that span the four proposed pulses of magmatism, which is more than adequate to resolve four pulses. However, the larger analytical uncertainties associated with the $^{40}\text{Ar}/^{39}\text{Ar}$ dates suggest a limit in this technique's resolving power.

To explore the analytical precision required to resolve the pulses of eruption purported to exist in Schoene et al. (2019), we constructed a synthetic dataset that consists of a stratigraphic section with cumulative erupted volume on the y-axis and time on the x-axis (Fig. 6). The dataset approximates the pulsed behavior observed in the U-Pb data – 4 pulses of eruption separated by relative lulls over a duration of ca. 800 ka. We then applied the same MCMC age model on these data, varying the analytical precision and calculating eruption rates as a function of time.

The predicted outcomes for the extreme endmembers are straightforward: with no uncertainty in the ages, the signal is clearly resolved and would still be so with many fewer datapoints. However, with ± 1 Ma precision, it is impossible to see any pulsed behavior, despite it being present in the underlying data. The results of this numerical experiment for various



analytical precisions spanning the range obtained by the geochronologic datasets show an increasing ability to resolve the four pulses of volcanism with increasing precision. For ± 50 ka, which approximates the uncertainty obtained in the U-Pb dataset, the four pulses are clearly resolvable (Fig. 6). Increasing uncertainty begins to smear this signal such that around ± 150 ka, it begins to be difficult to argue there's more than two pulses if any at all. By ± 200 ka, 70 ka less than the average uncertainty in the $^{40}\text{Ar}/^{39}\text{Ar}$ dataset, it is impossible to discern any signal except that of an approximately constant eruption rate (Fig. 6).

The above exercise shows that the current $^{40}\text{Ar}/^{39}\text{Ar}$ dataset is incapable of testing whether or not the Deccan Traps erupted at a constant rate, or with 2, 3, 4 or more pulses over the 800 ka lifespan of the LIP. This exercise does not prove that the pulsed eruption model derived from U-Pb geochronology is correct or complete, but simply shows that the $^{40}\text{Ar}/^{39}\text{Ar}$ dataset cannot be used to rigorously test it. Extending this line of reasoning, there are clearly finer-scale pulses within the Deccan Traps that the U-Pb data do not resolve. An endmember would be that of individual basalt flows, which are observed in modern volcanoes to erupt as pulses with timescales of days to months, but may take years to decades in the case of flood basalts (Self et al., 2014; Thordarson and Self, 1998). Similarly, redbole layers likely represent hiatuses in deposition of several thousand years on average (given at least 100 redboles exist through the stratigraphy), but the majority of them go undetected by the U-Pb data. This is consistent with the hiatuses represented by redboles being shorter than about half the average uncertainty in the U-Pb data, or 30 ka. This exercise highlights the need to acquire ever more precise geochronologic data, so as to better tease out finer-scale eruption dynamics in LIPs.

5. Systematic uncertainties: U-Pb and $^{40}\text{Ar}/^{39}\text{Ar}$ intercalibration.

Understanding and quantifying the systematic uncertainties between the $^{40}\text{Ar}/^{39}\text{Ar}$ and U-Pb dating methods have been major focuses in the effort to improve geochronologic intercalibration over the last two decades. (Renne et al., 1998) pointed out the $\sim 1\%$ difference in U-Pb and $^{40}\text{Ar}/^{39}\text{Ar}$ from rocks near the Permian-Triassic mass extinction event, and since then work has focused on examining and refining the ^{40}K decay constants and physical constants (such as $^{40}\text{K}/\text{K}$ and decay branching ratio; (Min et al., 2000; Villeneuve et al., 2000), testing the relative accuracy of the U decay constants (Mattinson, 2000, 2010; Schoene et al., 2006), and



developing better ages for high-K minerals used as neutron fluence monitors in $^{40}\text{Ar}/^{39}\text{Ar}$ geochronology (Kuiper et al., 2008; Kwon et al., 2002; Renne et al., 2010). Parallel efforts to
265 improve these systematic uncertainties have involved the intercalibration of rock samples dated by both the U-Pb and $^{40}\text{Ar}/^{39}\text{Ar}$ methods, which can help refine the accuracy and precision of each method (Machlus et al., 2020; Min et al., 2000; Renne et al., 2010; Schoene et al., 2006; Villeneuve et al., 2000). Ongoing experiments to remeasure the U decay constants will provide much needed additional data to test their presumed accuracy (Parsons-Davis et al., 2018).

270 Despite much progress towards intercalibrating these two chronometers, significant uncertainties remain that prevent integrating datasets at the precision required to inform LIP chronology. Arguably the most important remaining source of systematic uncertainty for Cenozoic samples is the adopted age of neutron fluence monitors used in $^{40}\text{Ar}/^{39}\text{Ar}$ geochronology. These monitors, or standards, are natural minerals whose prescribed ages
275 directly influence the calculated ages of samples. In the age range of the Cretaceous-Paleogene boundary, the Fish Canyon sanidine (FCs) is typically used, for which most $^{40}\text{Ar}/^{39}\text{Ar}$ labs have adopted the age of either 28.201 Ma (Kuiper et al., 2008) or 28.294 Ma (Fig. 7; Renne et al., 2011; Renne et al., 2010). This discrepancy scales roughly linearly into the ages of unknowns near the Cretaceous-Paleogene boundary, resulting in an age difference of ~200 ka.
280 The $^{40}\text{Ar}/^{39}\text{Ar}$ data from the Deccan Traps were normalized to the FCs date of 28.294 Ma (Renne et al., 2011), which has resulted in good overall agreement between the U-Pb and $^{40}\text{Ar}/^{39}\text{Ar}$ datasets for the Deccan Traps (Fig. 3) and estimates for the lower and upper C29r magnetic reversals. However, the youngest U-Pb zircon date from the Fish Canyon tuff is 28.196 ± 0.038 Ma (Wotzlav et al., 2013), in better agreement with the younger FCs age
285 estimate of Kuiper et al. (2008) and (Rivera et al., 2011) Fig. 7a). The recently developed Bayesian zircon eruption age estimator gives an age that also agrees with the Kuiper et al. (2008) estimate (Keller et al., 2018). This poses a significant problem: if the U-Pb age for eruption of the Fish Canyon tuff is correct, then the $^{40}\text{Ar}/^{39}\text{Ar}$ dates for the Deccan Traps and the Chicxulub impact become younger by ~200 ka (Fig. 7b); if the Renne et al (2011) age for the
290 FCs is correct (Fig. 3), then the datasets from the Deccan Traps agree well but would require the U-Pb data and several other estimates from the FC tuff to be significantly too young. While it is well known that zircons are susceptible to Pb-loss, causing them to yield U-Pb dates that are too young, the FC zircons were subjected to chemical abrasion that helps to mitigate Pb-loss (Mattinson, 2005). Importantly, the trends in zircon geochemistry and age observed by



295 Wotzlav et al. (2013) suggest that the age dispersion in that dataset reflects magmatic growth,
not Pb-loss.

There is no easy solution to this problem, and it does not affect the relative dates within
each system. Similarly, if the entire suite of systematic uncertainties for each system were to be
included (FCs standard age, decay constants for both U and ^{40}K , tracer uncertainties used in ID-
300 TIMS, and the physical constants of K; see summaries in (Condon et al., 2015; McLean et al.,
2015; Renne et al., 2011; Renne et al., 2010), the datasets would overlap within uncertainty
regardless of the choice of FCs age. However, the ideal scenario combining the U-Pb and
 $^{40}\text{Ar}/^{39}\text{Ar}$ dates from the Deccan Traps is premature, and evaluating the sources of apparent
disagreement between in absolute dates in the $^{40}\text{Ar}/^{39}\text{Ar}$ and U-Pb dates near the top of the
305 Ambenali Fm. is hampered.

6. Discussion and Conclusions.

Determining the rates of LIP magmatism is crucial for building models that explain in what ways
310 large scale volcanism can lead to mass extinction events and climate change. Without detailed
knowledge of the tempo of extrusion and intrusion, and how these two endmember magmatic
processes are distributed through time and space, we cannot expect to derive the rates of
volatile release that are the presumed driver of climate change and biosphere collapse. High
precision geochronology is an essential piece of this puzzle and is only just beginning to reveal
315 answers to these questions (Blackburn et al., 2013; Burgess and Bowring, 2015; Davies et al.,
2017; Kasbohm and Schoene, 2018; Mahood and Benson, 2017), but much remains to be
done. Determining and maximizing the precision and accuracy of dates for erupted volumes of
magma will continue to be a challenge and require integration of geochronology with geologic,
geochemical, geophysical, and petrological data. The above analysis does not address most
320 aspects of this integration and assumes that the $^{40}\text{Ar}/^{39}\text{Ar}$ and U-Pb datasets recently published
for the Deccan Traps are accurate at their stated precision. Continued work addressing both
analytical and geological uncertainties on determining basalt eruption ages from geochronology
is necessary to validate that assumption. The $^{40}\text{Ar}/^{39}\text{Ar}$ and U-Pb datasets for the Deccan Traps
from Sprain et al. (2019) and Schoene et al. (2019) pose a unique opportunity to do this
325 because both studies sample the LIP with unprecedented resolution, and push the limits of
precision and accuracy for each method.



We have highlighted here several issues with the way the $^{40}\text{Ar}/^{39}\text{Ar}$ data were used to build a model for eruption rates of the Deccan Traps, and do so because the model has been reproduced in summaries of the two articles (Burgess, 2019), the popular media (e.g., Voosen, 330 2019), and in subsequent presentations and papers discussing these datasets (Henehan et al., 2019; Hull et al., 2020; Linzmeier et al., 2020; Milligan et al., 2019; Montanari and Coccioni, 2019). The potential fallout of these misunderstandings is that it risks painting a picture among non-geochronologists that the U-Pb and $^{40}\text{Ar}/^{39}\text{Ar}$ methods cannot agree on the eruption history of the Deccan Traps and that the geological community should be skeptical of geochronology in 335 general. We have shown that, systematic uncertainties aside, the $^{40}\text{Ar}/^{39}\text{Ar}$ dataset for the Deccan Traps determined by Sprain et al. (2019) is largely compatible with the U-Pb dataset presented in Schoene et al. (2019), which is an achievement for geochronology and should be celebrated. However, we also show that one of the key suggestions in Sprain et al. (2019), that eruption rates increased following the Chicxulub impact, is not supported by either dataset given 340 the current age constraints for the impact. This relationship could be further tested by, for example, additional geochronology on the Deccan Traps, reproducing the current U-Pb date for the impact, and/or nailing down U-Pb and $^{40}\text{Ar}/^{39}\text{Ar}$ intercalibration such that the U-Pb record of the Deccan could be compared to the $^{40}\text{Ar}/^{39}\text{Ar}$ date for the impact.

To be clear, this paper is not meant to suggest that the pulsed eruption model based on 345 the U-Pb geochronology is necessarily correct. This model should be treated as a working hypothesis that needs to be tested further with additional high-precision geochronology on samples that can test the stratigraphic correlations used in Schoene et al. (2019); also, continued work to produce more robust estimates for eruption ages from complex zircon datasets is needed (Galeotti et al., 2019; Keller et al., 2018; Schoene et al., 2010). Additional 350 geochronology is also needed to provide a broader perspective on Deccan volcanism regionally (Knight et al., 2003; Eddy et al., in press; Parisio et al., 2016; Schöbel et al., 2014; Sheth et al., 2019). These data must be combined with samples and geophysical data that characterize the intrusive history of the Traps. Finally, to better understand the potential climatic impact of Deccan magmatism, more work must to be done to understand the history of volatile release 355 and whether or not this correlates with the eruptive history (Black and Gibson, 2019; Self et al., 2008; Svensen et al., 2010; Svensen et al., 2004). But key to this work is that we, as geochronologists, set the standard for uncertainty assessment in data collection and age interpretation as well as how these data are used to generate eruption age models that the greater geoscience community can leverage in their own research.



360 **Acknowledgements**

Gerta Keller, Thierry Adatte, and Syed Khadri are thanked for ongoing collaboration on research related to the Deccan Traps, which formed the basis for this study.

365



References

- Alvarez, L. W., Alvarez, W., Asaro, F., and Michel, H. V., 1980, Extraterrestrial cause for the
370 Cretaceous-Tertiary extinction: *Science*, v. 208, no. 4448, p. 1095-1108.
- Beane, J. E., Turner, C. A., Hooper, P. R., Subbarao, K. V., and Walsh, J. N., 1986,
Stratigraphy, composition and form of the Deccan Basalts, Western Ghats, India:
Bulletin of Volcanology, v. 48, no. 1, p. 61-83.
- Blaauw, M., and Christen, J. A., 2011, Flexible paleoclimate age-depth models using an
375 autoregressive gamma process: *Bayesian analysis*, v. 6, no. 3, p. 457-474.
- Black, B. A., and Gibson, S. A., 2019, Deep Carbon and the Life Cycle of Large Igneous
Provinces: *Elements*, v. 15, no. 5, p. 319-324.
- Black, B. A., and Manga, M., 2017, Volatiles and the tempo of flood basalt magmatism: *Earth
and Planetary Science Letters*, v. 458, p. 130-140.
- 380 Blackburn, T. J., Olsen, P. E., Bowring, S. A., McLean, N. M., Kent, D. V., Puffer, J., McHone,
G., Rasbury, E. T., and Et-Touhami, M., 2013, Zircon U-Pb Geochronology Links the
End-Triassic Extinction with the Central Atlantic Magmatic Province: *Science*, v. 340, no.
6135, p. 941-945.
- Bond, D. P. G., and Wignall, P. B., 2014, Large igneous provinces and mass extinctions: An
385 update: *Geological Society of America Special Papers*, v. 505, p. 29-55.
- Burgess, S., 2019, Deciphering mass extinction triggers: *Science*, v. 363, no. 6429, p. 815-816.
- Burgess, S. D., and Bowring, S. A., 2015, High-precision geochronology confirms voluminous
magmatism before, during, and after Earth's most severe extinction: *Science advances*,
v. 1, no. 7, p. e1500470.
- 390 Byrnes, J. S., and Karlstrom, L., 2018, Anomalous K-Pg-aged seafloor attributed to impact-
induced mid-ocean ridge magmatism: *Science advances*, v. 4, no. 2, p. eaao2994.
- Chenet, A.-L., Courtillot, V., Fluteau, F., Gérard, M., Quidelleur, X., Khadri, S. F. R., Subbarao,
K. V., and Thordarson, T., 2009, Determination of rapid Deccan eruptions across the
Cretaceous-Tertiary boundary using paleomagnetic secular variation: 2. Constraints
395 from analysis of eight new sections and synthesis for a 3500-m-thick composite section:
Journal of Geophysical Research, v. 114, no. B6.
- Chenet, A.-L., Fluteau, F., Courtillot, V., Gérard, M., and Subbarao, K. V., 2008, Determination
of rapid Deccan eruptions across the Cretaceous-Tertiary boundary using
paleomagnetic secular variation: Results from a 1200-m-thick section in the
400 Mahabaleshwar escarpment: *Journal of Geophysical Research*, v. 113, no. B4.
- Clyde, W. C., Ramezani, J., Johnson, K. R., Bowring, S. A., and Jones, M. M., 2016, Direct
high-precision U-Pb geochronology of the end-Cretaceous extinction and calibration of
Paleocene astronomical timescales: *Earth and Planetary Science Letters*, v. 452, p. 272-
280.
- 405 Condon, D., Schoene, B., McLean, N., Bowring, S., and Parrish, R., 2015, Metrology and
traceability of U-Pb isotope dilution geochronology (EARTHTIME Tracer Calibration Part
I): *Geochimica et Cosmochimica Acta*, v. 164, p. 464-480.
- Courtillot, V., Besse, J., Vandamme, D., Montigny, R., Jaeger, J.-J., and Cappetta, H., 1986,
Deccan flood basalts at the Cretaceous/Tertiary boundary?: *Earth and Planetary
410 Science Letters*, v. 80, no. 3-4, p. 361-374.
- Courtillot, V., Feraud, G., Maluski, H., Vandamme, D., Moreau, M. G., and Besse, J., 1988,
Deccan flood basalts and the Cretaceous/Tertiary boundary: *Nature*, v. 333, no. 6176, p.
843-846.



- 415 Davies, J., Marzoli, A., Bertrand, H., Youbi, N., Ernesto, M., and Schaltegger, U., 2017, End-Triassic mass extinction started by intrusive CAMP activity: *Nature communications*, v. 8, p. 15596.
- Eddy, M. P., Schoene, B., Samperton, K. M., Keller, G., Adatte, T., and Khadri, S. F. R., in press, U-Pb zircon age constraints on the earliest eruptions of the Deccan Large Igneous Province, Malwa Plateau, India: *Earth Plan. Sci. Lett.*, p. 10.1016/j.epsl.2020.116249.
- 420 Ernst, R. E., and Youbi, N., 2017, How Large Igneous Provinces affect global climate, sometimes cause mass extinctions, and represent natural markers in the geological record: *Palaeogeography, Palaeoclimatology, Palaeoecology*, v. 478, p. 30-52.
- 425 Galeotti, S., Sahy, D., Agnini, C., Condon, D., Fornaciari, E., Francescone, F., Giusberti, L., Pálike, H., Spofforth, D. J. A., and Rio, D., 2019, Astrochronology and radio-isotopic dating of the Alano di Piave section (NE Italy), candidate GSSP for the Priabonian Stage (late Eocene): *Earth and Planetary Science Letters*, v. 525, p. 115746.
- Haslett, J., and Parnell, A., 2008, A simple monotone process with application to radiocarbon-dated depth chronologies: *Journal of the Royal Statistical Society: Series C (Applied Statistics)*, v. 57, no. 4, p. 399-418.
- 430 Henehan, M. J., Ridgwell, A., Thomas, E., Zhang, S., Alegret, L., Schmidt, D. N., Rae, J. W. B., Witts, J. D., Landman, N. H., Greene, S. E., Huber, B. T., Super, J. R., Planavsky, N. J., and Hull, P. M., 2019, Rapid ocean acidification and protracted Earth system recovery followed the end-Cretaceous Chicxulub impact: *Proceedings of the National Academy of Sciences*, v. 116, no. 45, p. 22500.
- 435 Hildebrand, A. R., Penfield, G. T., Kring, D. A., Pilkington, M., Camargo Z, A., Jacobsen, S. B., and Boynton, W. V., 1991, Chicxulub crater: a possible Cretaceous/Tertiary boundary impact crater on the Yucatan Peninsula, Mexico: *Geology*, v. 19, no. 9, p. 867-871.
- 440 Hull, P. M., Bornemann, A., Penman, D. E., Henehan, M. J., Norris, R. D., Wilson, P. A., Blum, P., Alegret, L., Batenburg, S. J., and Bown, P. R., 2020, On impact and volcanism across the Cretaceous-Paleogene boundary: *Science*, v. 367, no. 6475, p. 266-272.
- Kale, V. S., Dole, G., Shandilya, P., and Pande, K., 2020, Stratigraphy and correlations in Deccan Volcanic Province, India: *Quo vadis?: Bulletin*, v. 132, no. 3-4, p. 588-607.
- 445 Kasbohm, J., and Schoene, B., 2018, Rapid eruption of the Columbia River flood basalt and correlation with the mid-Miocene climate optimum: *Science Advances*, v. 4, no. 9.
- Kasbohm, J., Schoene, B., and Burgess, S. D., in press, Radiometric constraints on the timing, tempo, and effects of large igneous province emplacement: *AGU special volume*.
- Keller, C. B., 2018, *Chron.jl: A Bayesian framework for integrated eruption age and age-depth modelling*. <https://doi.org/10.17605/osf.io/TQX3F>.
- 450 Keller, C. B., Schoene, B., and Samperton, K. M., 2018, A stochastic sampling approach to zircon eruption age interpretation: *Geochemical Perspectives Letters*, v. 8, p. 31-35.
- Keller, G., Adatte, T., Gardin, S., Bartolini, A., and Bajpai, S., 2008, Main Deccan volcanism phase ends near the K-T boundary: Evidence from the Krishna-Godavari Basin, SE India: *Earth and Planetary Science Letters*, v. 268, no. 3-4, p. 293-311.
- 455 Kerr, A. C., and Ward, P. D., 2019, A Dominant Role for The K-Pg Impact, Aug. 17, 2019: <https://science.sciencemag.org/content/363/6429/862/tab-e-letters>.
- Knight, K. B., Renne, P. R., Halkett, A., and White, N., 2003, ⁴⁰Ar/³⁹Ar dating of the Rajahmundry Traps, Eastern India and their relationship to the Deccan Traps: *Earth and Planetary Science Letters*, v. 208, no. 1-2, p. 85-99.
- 460 Kuiper, K. F., Deino, A., Hilgen, F. J., Krijgsman, W., Renne, P. R., and Wijbrans, J. R., 2008, Synchronizing rocks clocks of Earth history: *Science*, v. 320, p. 500-504, DOI: 510.1126/science.1154339



- 465 Kwon, J., Min, K., Bickel, P. J., and Renne, P. R., 2002, Statistical methods for jointly estimating
the decay constant of ^{40}K and the age of a dating standard: *Mathematical Geology*, v.
34, no. 4, p. 457-474.
- Linzmeier, B. J., Jacobson, A. D., Sageman, B. B., Hurtgen, M. T., Ankney, M. E., Petersen, S.
V., Tobin, T. S., Kitch, G. D., and Wang, J., 2020, Calcium isotope evidence for
environmental variability before and across the Cretaceous-Paleogene mass extinction:
Geology, v. 48, no. 1, p. 34-38.
- 470 Machlus, M. L., Shea, E. K., Hemming, S. R., Ramezani, J., and Rasbury, E. T., 2020, An
assessment of sanidine from the Fire Clay tonstein as a Carboniferous $^{40}\text{Ar}/^{39}\text{Ar}$
monitor standard and for inter-method comparison to U-Pb zircon geochronology:
Chemical Geology, v. 539, p. 119485.
- 475 Mahood, G. A., and Benson, T. R., 2017, Using $^{40}\text{Ar}/^{39}\text{Ar}$ ages of intercalated silicic tuffs to
date flood basalts: Precise ages for Steens Basalt Member of the Columbia River Basalt
Group: *Earth and Planetary Science Letters*, v. 459, p. 340-351.
- Marzoli, A., Callegaro, S., Dal Corso, J., Davies, J. H., Chiaradia, M., Youbi, N., Bertrand, H.,
Reisberg, L., Merle, R., and Jourdan, F., 2018, The Central Atlantic magmatic province
(CAMP): a review, *The Late Triassic World*, Springer, p. 91-125.
- 480 Mattinson, J. M., 2000, Revising the "gold standard" – the uranium decay constants of Jaffey et
al., 1971: *Eos Trans. AGU, Spring Meet. Suppl.*, Abstract V61A-02.
- , 2005, Zircon U-Pb chemical-abrasion ("CA-TIMS") method: combined annealing and multi-
step dissolution analysis for improved precision and accuracy of zircon ages: *Chem.
Geol.*, v. 220, no. 1-2, p. 47-56.
- 485 -, 2010, Analysis of the relative decay constants of ^{235}U and ^{238}U by multi-step CA-TIMS
measurements of closed-system natural zircon samples: *Chemical Geology*, v. 275, no.
3-4, p. 186-198.
- McLean, D. M., 1985, Deccan Traps mantle degassing in the terminal Cretaceous marine
extinctions: *Cretaceous Research*, v. 6, no. 3, p. 235-259.
- 490 McLean, N. M., Condon, D. J., Schoene, B., and Bowring, S. A., 2015, Evaluating uncertainties
in the calibration of isotopic reference materials and multi-element isotopic tracers
(EARTHTIME Tracer Calibration Part II): *Geochimica et Cosmochimica Acta*, v. 164, p.
481-501.
- 505 Milligan, J. N., Royer, D. L., Franks, P. J., Upchurch, G. R., and McKee, M. L., 2019, No
evidence for a large atmospheric CO_2 spike across the Cretaceous-Paleogene
boundary: *Geophysical Research Letters*, v. 46, no. 6, p. 3462-3472.
- Min, K., Mundil, R., Renne, P. R., and Ludwig, K. R., 2000, A test for systematic errors in
 $^{40}\text{Ar}/^{39}\text{Ar}$ geochronology through comparison with U-Pb analysis of a 1.1 Ga rhyolite:
Geochim. Cosmochim. Acta, v. 64, p. 73-98.
- 500 Minnis, P., Harrison, E. F., Stowe, L. L., Gibson, G., Denn, F. M., Doelling, D., and Smith, W.,
1993, Radiative climate forcing by the Mount Pinatubo eruption: *Science*, v. 259, no.
5100, p. 1411-1415.
- Mitchell, C., and Widdowson, M., 1991, A geological map of the southern Deccan Traps, India
and its structural implications: *Journal of the Geological Society*, v. 148, no. 3, p. 495-
505.
- 505 Montanari, A., and Coccioni, R., 2019, The serendipitous discovery of an extraterrestrial iridium
anomaly at the Cretaceous-Paleogene boundary in Gubbio and the rise of a far-reaching
theory: *Bollettino della Società Paleontologica Italiana*, v. 58, no. 1, p. 78.
- 510 Parisio, L., Jourdan, F., Marzoli, A., Melluso, L., Sethna, S. F., and Bellieni, G., 2016, $^{40}\text{Ar}/^{39}\text{Ar}$
ages of alkaline and tholeiitic rocks from the northern Deccan Traps: implications for



- magmatic processes and the K–Pg boundary: *Journal of the Geological Society*, v. 173, no. 4, p. 679-688.
- 515 Parnell, A. C., Buck, C. E., and Doan, T. K., 2011, A review of statistical chronology models for high-resolution, proxy-based Holocene palaeoenvironmental reconstruction: *Quaternary Science Reviews*, v. 30, no. 21, p. 2948-2960.
- Parsons-Davis, T., Wimpenny, J., Keller, C. B., Thomas, K., Samperton, K. M., Renne, P. R., Mundil, R., Moody, K., Knight, K., and Kristo, M. J., 2018, New measurement of the ^{238}U decay constant with inductively coupled plasma mass spectrometry: *Journal of Radioanalytical and Nuclear Chemistry*, v. 318, no. 1, p. 711-721.
- 520 Rampino, M. R., and Caldeira, K., 1992, Antipodal hotspot pairs on the Earth: *Geophysical research letters*, v. 19, no. 20, p. 2011-2014.
- Renne, P. R., Balco, G., Ludwig, K. R., Mundil, R., and Min, K., 2011, Response to the comment by WH Schwarz et al. on “Joint determination of 40K decay constants and $^{40}\text{Ar}/^{39}\text{Ar}$ geochronology” by PR Renne et al.(2010): *Geochimica et Cosmochimica Acta*, v. 75, no. 17, p. 5097-5100.
- 525 Renne, P. R., Deino, A. L., Hilgen, F. J., Kuiper, K. F., Mark, D. F., Mitchell, W. S., 3rd, Morgan, L. E., Mundil, R., and Smit, J., 2013, Time scales of critical events around the Cretaceous-Paleogene boundary: *Science*, v. 339, no. 6120, p. 684-687.
- 530 Renne, P. R., Karner, D. B., and Ludwig, K. R., 1998, Absolute ages aren't exactly: *Science*, v. 282, p. 1840-1841.
- Renne, P. R., Mundil, R., Balco, G., Min, K., and Ludwig, K. R., 2010, Joint determination of 40K decay constants and $^{40}\text{Ar}/^{39}\text{Ar}$ for the Fish Canyon sanidine standard, and improved accuracy for $^{40}\text{Ar}/^{39}\text{Ar}$ geochronology: *Geochimica et Cosmochimica Acta*, v. 74, no. 18, p. 5349-5367.
- 535 Renne, P. R., Sprain, C. J., Richards, M. A., Self, S., Vanderkluyzen, L., and Pande, K., 2015, State shift in Deccan volcanism at the Cretaceous-Paleogene boundary, possibly induced by impact: *Science*, v. 350, no. 6256, p. 76-78.
- 540 Ricci, J., Quidelleur, X., Pavlov, V., Orlov, S., Shatsillo, A., and Courtillot, V., 2013, New $^{40}\text{Ar}/^{39}\text{Ar}$ and K–Ar ages of the Viluy traps (Eastern Siberia): further evidence for a relationship with the Frasnian–Famennian mass extinction: *Palaeogeography, Palaeoclimatology, Palaeoecology*, v. 386, p. 531-540.
- 545 Richards, M. A., Alvarez, W., Self, S., Karlstrom, L., Renne, P. R., Manga, M., Sprain, C. J., Smit, J., Vanderkluyzen, L., and Gibson, S. A., 2015, Triggering of the largest Deccan eruptions by the Chicxulub impact: *Geological Society of America Bulletin*, v. 127, no. 11-12, p. 1507-1520.
- Rivera, T. A., Storey, M., Zeeden, C., Hilgen, F. J., and Kuiper, K., 2011, A refined astronomically calibrated $^{40}\text{Ar}/^{39}\text{Ar}$ age for Fish Canyon sanidine: *Earth and Planetary Science Letters*, v. 311, no. 3-4, p. 420-426.
- 550 Robock, A., 2000, Volcanic eruptions and climate: *Reviews of geophysics*, v. 38, no. 2, p. 191-219.
- Schöbel, S., de Wall, H., Ganerød, M., Pandit, M. K., and Rolf, C., 2014, Magnetostratigraphy and ^{40}Ar – ^{39}Ar geochronology of the Malwa Plateau region (Northern Deccan Traps), central western India: Significance and correlation with the main Deccan Large Igneous Province sequences: *Journal of Asian Earth Sciences*, v. 89, no. 0, p. 28-45.
- 555 Schoene, B., Crowley, J. L., Condon, D. C., Schmitz, M. D., and Bowring, S. A., 2006, Reassessing the uranium decay constants for geochronology using ID-TIMS U-Pb data: *Geochim. Cosmochim. Acta*, v. 70, p. 426-445.



- 560 Schoene, B., Eddy, M. P., Samperton, K. M., Keller, C. B., Keller, G., Adatte, T., and Khadri, S. F. R., 2019, U-Pb constraints on pulsed eruption of the Deccan Traps across the end-Cretaceous mass extinction: *Science*, v. 363, no. 6429, p. 862.
- Schoene, B., Guex, J., Bartolini, A., Schaltegger, U., and Blackburn, T. J., 2010, Correlating the end-Triassic mass extinction and flood basalt volcanism at the 100,000-year level: *Geology*, v. 38, p. 387-390. DOI: 310.1130/G30683.30681.
- 565 Schoene, B., Samperton, K. M., Eddy, M. P., Keller, G., Adatte, T., Bowring, S. A., Khadri, S. F., and Gertsch, B., 2015, U-Pb geochronology of the Deccan Traps and relation to the end-Cretaceous mass extinction: *Science*, v. 347, no. 6218, p. 182-184.
- Schulte, P., Alegret, L., Arenillas, I., Arz, J. A., Barton, P. J., Bown, P. R., Bralower, T. J., Christeson, G. L., Claeys, P., and Cockell, C. S., 2010, The Chicxulub asteroid impact and mass extinction at the Cretaceous-Paleogene boundary: *Science*, v. 327, no. 5970, p. 1214-1218.
- 570 Self, S., Blake, S., Sharma, K., Widdowson, M., and Sephton, S., 2008, Sulfur and chlorine in late Cretaceous Deccan magmas and eruptive gas release: *Science*, v. 319, no. 5870, p. 1654-1657.
- 575 Self, S., Schmidt, A., and Mather, T. A., 2014, Emplacement characteristics, time scales, and volcanic gas release rates of continental flood basalt eruptions on Earth: *Geological Society of America Special Papers*, v. 505, p. 319-337.
- Shellnutt, J. G., Denyszyn, S. W., and Mundil, R., 2012, Precise age determination of mafic and felsic intrusive rocks from the Permian Emeishan large igneous province (SW China): *Gondwana Research*, v. 22, no. 1, p. 118-126.
- 580 Sheth, H., Vanderkluyzen, L., Demonterova, E. I., Ivanov, A. V., and Savatenkov, V. M., 2019, Geochemistry and $^{40}\text{Ar}/^{39}\text{Ar}$ geochronology of the Nandurbar-Dhule mafic dyke swarm: Dyke-sill-flow correlations and stratigraphic development across the Deccan flood basalt province: *Geological Journal*, v. 54, no. 1, p. 157-176.
- 585 Smit, J., and Hertogen, J., 1980, An extraterrestrial event at the Cretaceous–Tertiary boundary: *Nature*, v. 285, no. 5762, p. 198-200.
- Sprain, C. J., Renne, P. R., Clemens, W. A., and Wilson, G. P., 2018, Calibration of chron C29r: New high-precision geochronologic and paleomagnetic constraints from the Hell Creek region, Montana: *Geological Society of America Bulletin*.
- 590 Sprain, C. J., Renne, P. R., Vanderkluyzen, L., Pande, K., Self, S., and Mittal, T., 2019, The eruptive tempo of Deccan volcanism in relation to the Cretaceous-Paleogene boundary: *Science*, v. 363, no. 6429, p. 866-870.
- Subbarao, K., Bodas, M., Khadri, S., and Beane, J., 2000, Penrose Deccan 2000, Field Excursion Guide to the Western Deccan Basalt Province: Penrose Field Guides, B. Geological Society of India, ed.
- 595 Svensen, H., Planke, S., and Corfu, F., 2010, Zircon dating ties NE Atlantic sill emplacement to initial Eocene global warming: *Journal of the Geological Society*, v. 167, no. 3, p. 433-436.
- 600 Svensen, H., Planke, S., Malthe-Sørenssen, A., Jamtveit, B., Myklebust, R., Eidem, T. R., and Rey, S. S., 2004, Release of methane from a volcanic basin as a mechanism for initial Eocene global warming: *Nature*, v. 429, no. 6991, p. 542.
- Thordarson, T., and Self, S., 1998, The Roza Member, Columbia River Basalt Group: A gigantic pahoehoe lava flow field formed by endogenous processes?: *Journal of Geophysical Research: Solid Earth*, v. 103, no. B11, p. 27411-27445.
- 605 Villeneuve, M., Sandeman, H. A., and Davis, W. J., 2000, A method for intercalibration of U-Th-Pb and ^{40}Ar - ^{39}Ar ages in the Phanerozoic: *Geochimica et Cosmochimica Acta*, v. 64, no. 23, p. 4017-4030.



- Voosen, P., 2019, Did volcanic eruptions help kill off the dinosaurs?:
<https://www.sciencemag.org/news/2019/02/did-volcanic-eruptions-help-kill-dinosaurs>.
- 610 Wright, A. J., Edwards, R. J., van de Plasche, O., Blaauw, M., Parnell, A., van der Borg, K., de
Jong, A., Selby, K. A., Roe, H., and Black, S., 2017, Reconstructing the accumulation
history of a saltmarsh sediment core: which age-depth model is best?: Quaternary
Geochronology, p. 35-67.

615

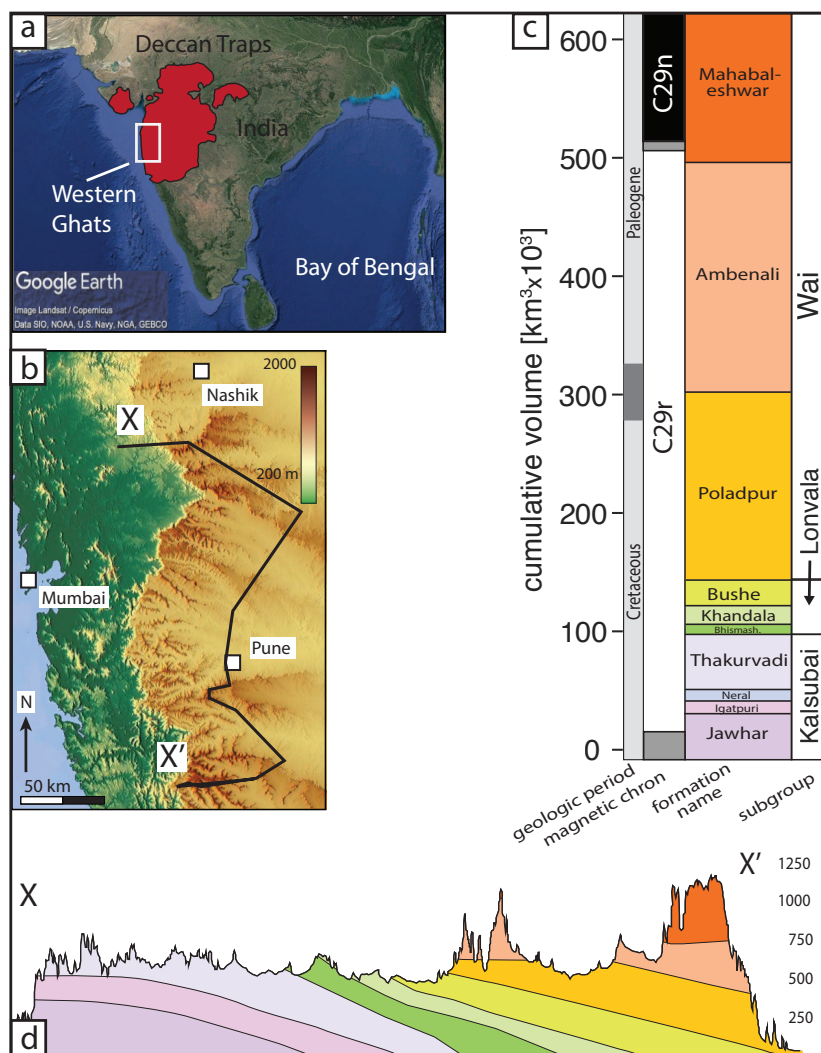


Fig. 1: Geography and stratigraphy of the Deccan Traps in the Western Ghats Region. a) Map of India (© Google Earth), showing in red the footprint of the Deccan Traps; white box indicates the study area, called the western Ghats, enlarged in (b). b) Colored relief map (© OpenStreetMap contributors 2020. Distributed under a Creative Commons BY-SA License) of the Western Ghats showing several cities and cross-section line from (d). c) Stratigraphic column of the major basalt unit subdivisions in the Western Ghats. Stratigraphy measured as cumulative volume, using the volume model for each formation from (Richards et al., 2015), which was used in both Schoene et al. (2019) and Sprain et al. (2019). d) Cross section through the Western Ghats. Cross-section line chosen to go through the sampling sites in Schoene et al. (2019). All figures modified from Schoene et al. (2015), Schoene et al. (2019), and references therein.

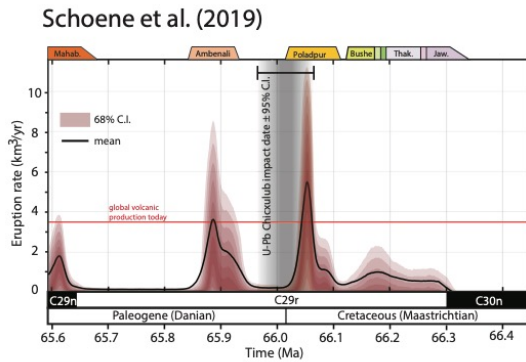


Fig. 2. Eruption rate model for the Deccan Traps, based on U-Pb geochronology. (A) Results from the MCMC algorithm used to generate the age model in Fig. 1, converted to a probabilistic volumetric eruption rate for the Deccan Traps shown with contours up to 68% credible intervals. The U-Pb date for the Chicxulub impact is the same as in Fig. 1. Total global volcanic productivity (~3–4 km³/year) includes mid-ocean ridges and volcanic arcs (28).

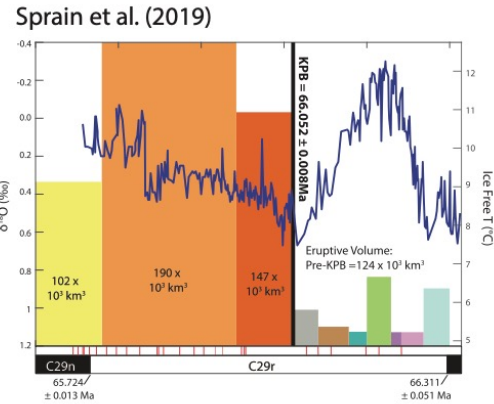


Fig. 4. Eruptive flux and climatic changes. Correlation of Deccan eruptive fluxes to benthic $\delta^{18}\text{O}$ data from Ocean Drilling Program site 1262 (blue line) [published in (15)]. Colored blocks represent eruptive fluxes, where color indicates the formation per Fig. 2; horizontal length indicates the approximate duration; and height is scaled by eruptive volume as calculated in (17). Red lines mark the locations of redboles taken from (9, 10, 33, 34). Ages shown for the KPB, C29r/C29n, and C30n/C29r reversals are ⁴⁰Ar/³⁹Ar ages from (25). T, temperature.

Fig. 2: Published eruption rates for the Deccan Traps. Figures illustrating eruption rate, or
 630 flux, reproduced from Fig. 2A of Schoene et al. (2019), left, and Fig. 4 of Sprain et al. (2019),
 right. Captions beneath illustrations are exactly as printed in those publications. Uncertainties in
 Sprain et al. are 1sigma. Fig. 2A from Schoene et al. (2019) is modified here to exclude Fig. 2B
 635 but keep the x-axis. References from captions (numbers in italics) can be found in the original
 publications. Note that colors used for the different formations are not the same in each figure,
 640 but the stratigraphic order is the same from right to left. The main point made in the text from
 this paper is that the units on the y-axis in the Schoene et al. (2019) figure are in [km³/a], which
 are the units of a rate or flux; the units on the y-axis in the Sprain et al. (2019) figure for the
 Deccan portion are [km³], which are not a flux, and therefore the figure does not represent an
 eruption rate or flux as stated.

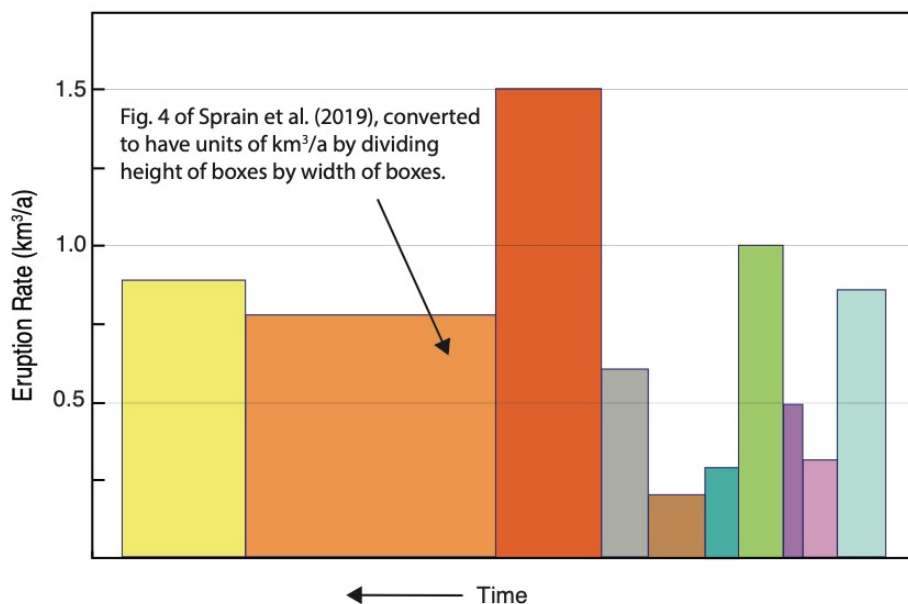


Fig. 3: Recalculated eruption rates from Fig. 4 of Sprain et al. (2019). Original figure was converted to an eruption rate by dividing the total volume of each formation (the heights in their Fig. 4), by their estimated durations for each formation, to give units of km^3/a . Time on the x-axis, and color and width of each box is left as from their original figure. See Fig. 4 of this paper for probabilistic eruption rates.

645

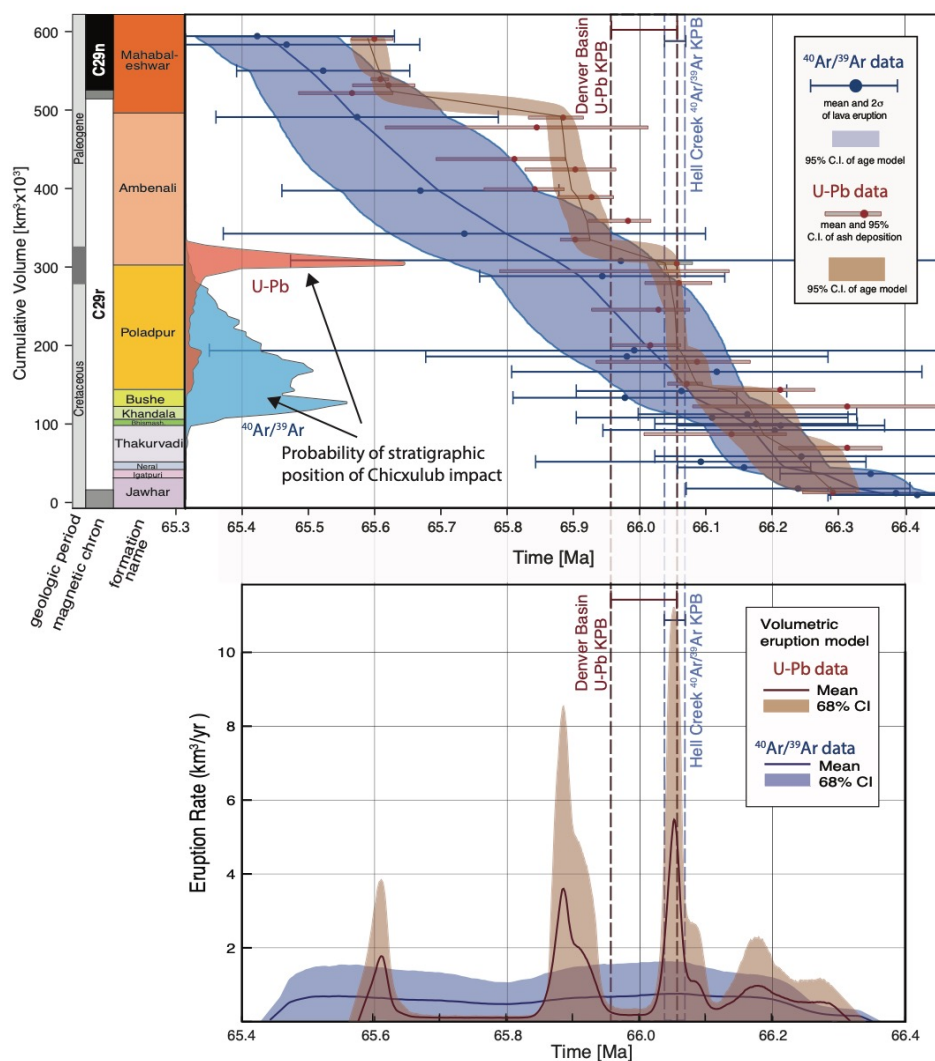
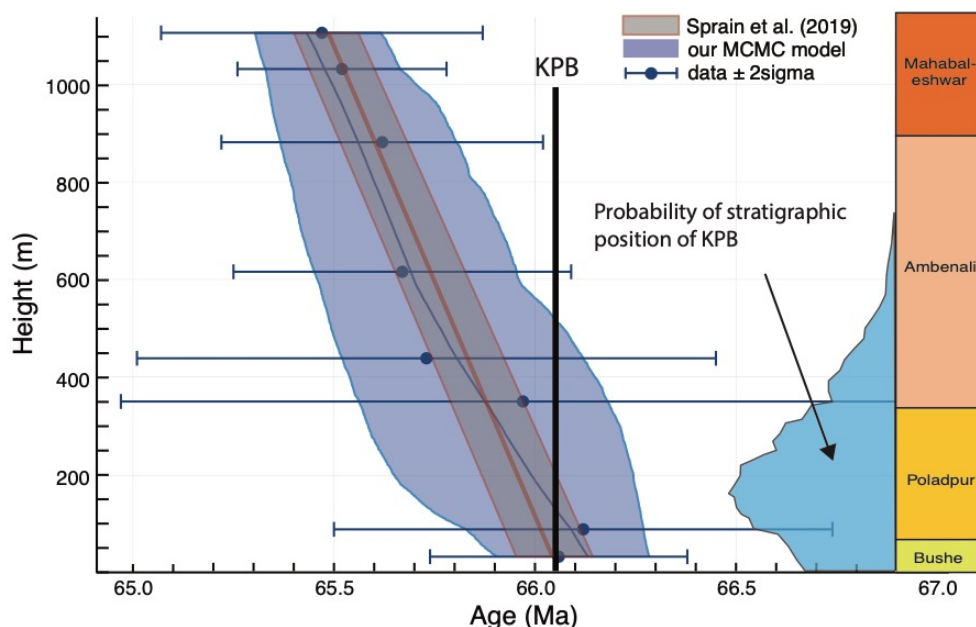


Fig. 4: Age models and eruption rates for the Deccan Traps. Age models and eruptions rates produced using geochronologic data from Schoene et al. (2019; red) and Sprain et al. (2019; blue), using the same methods as described in Schoene et al. (2019). Data and model for Schoene et al. (2019) are identical to those in the original publication. Note the units on the stratigraphy in the top panel are cumulative km^3 , not m, and so the slope of the age models are km^3/a , which is plotted in the lower panel. Volume model is from Richards et al. (2015).
 650
 655 Stratigraphic heights for the Sprain et al. (2019) samples are taken from their Fig. 2. Also plotted is the probability of the stratigraphic position of the Chicxulub impact as calculated during the MCMC age modeling by querying where an accepted age model intersects an age for the KPg. U-Pb age model is compared to U-Pb KPg date from Clyde et al., (2016); $^{40}\text{Ar}/^{39}\text{Ar}$ age model is compared to $^{40}\text{Ar}/^{39}\text{Ar}$ KPg date from (Sprain et al., 2018).

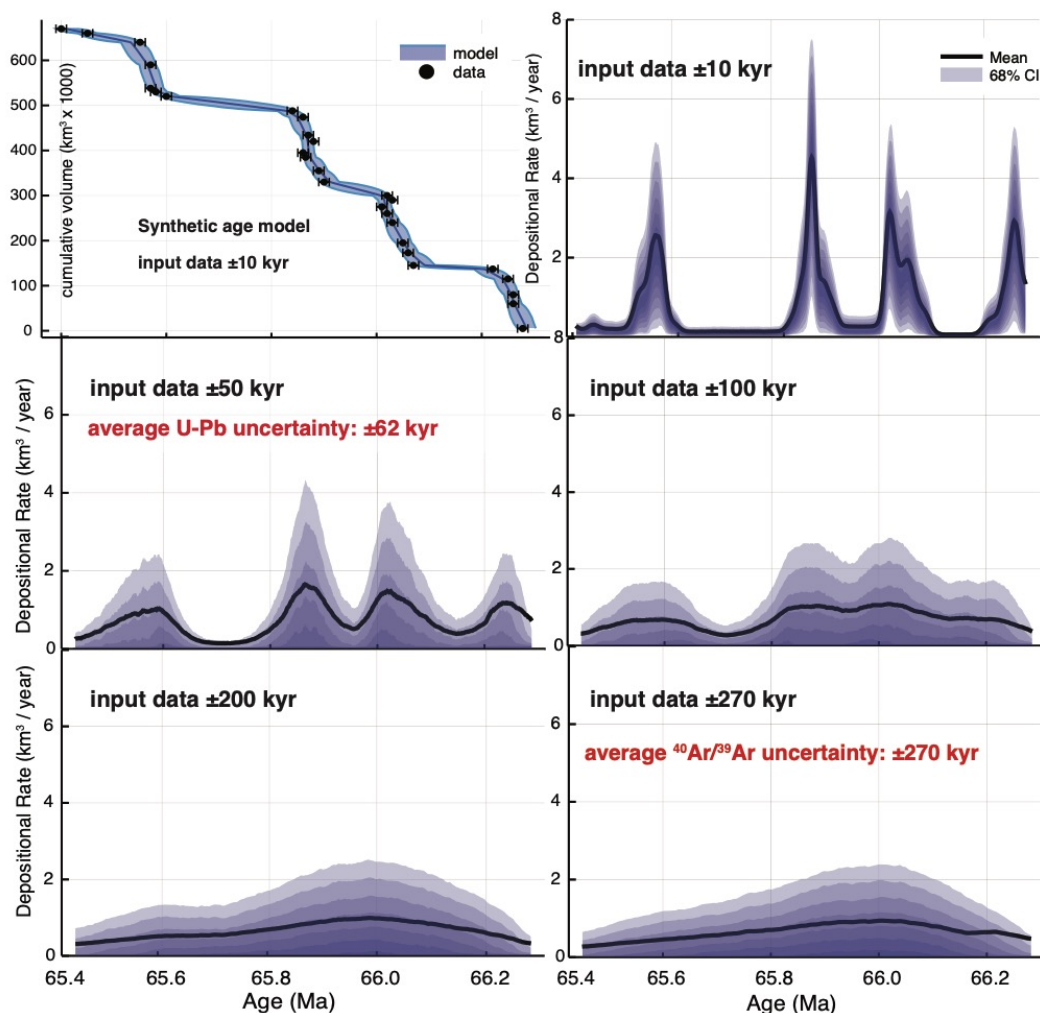


660

Fig. 5: A reanalysis of an $^{40}\text{Ar}/^{39}\text{Ar}$ age model using data from a single stratigraphic section. Carried out on the Ambenali Ghat, as per Sprain et al. (2019). Results with 95% CI from our MCMC algorithm are shown over top the model presented in Sprain et al. (2019), using the freely available Bayesian MCMC model Bacon (Blaauw and Christen, 2011). The difference in the results arises from assumptions about deposition rates imposed by Bacon, resulting in smaller uncertainties. Formation stratigraphy is plotted on the right, using the color-scheme from Schoene et al. (2019). To the left of stratigraphic column is plotted a histogram of the possible stratigraphic height of the Chicxulub impact (KPB) using the $^{40}\text{Ar}/^{39}\text{Ar}$ Deccan data and the $^{40}\text{Ar}/^{39}\text{Ar}$ date for the impact (KPB) from Sprain et al. (2018). A large portion of the histogram would plot beneath 0 meters height, but cannot be calculated accurately. Note these results contrast significantly from the conclusion in Sprain et al. (2019), who conclude that the KPB falls at the Bushe-Poladpur contact.

665

670



675 **Fig. 6: Synthetic dataset subjected to MCMC age modeling to test the age precision**
necessary to resolve pulses in eruptions. Upper left shows the dataset, meant to
approximate the age model of Schoene et al. (2019), but shown here with negligible
uncertainties (± 10 ka 2σ). Other panels show model outputs for eruption rates generated
680 for different 2σ uncertainties on the input data themselves (i.e., uncertainties on “data” from
upper left panel). The results indicate that a threshold of precision is required for geochronology
to resolve pulses and hiatuses of given durations. Also shown in red are the average reported
 2σ uncertainties on eruption ages from the U-Pb dataset of Schoene et al. (2019) and the
 $^{40}\text{Ar}/^{39}\text{Ar}$ dataset from Sprain et al. (2019). The point is that the lower precision $^{40}\text{Ar}/^{39}\text{Ar}$ dataset
cannot possibly test the hiatus and pulse model observed by the U-Pb dataset.

685

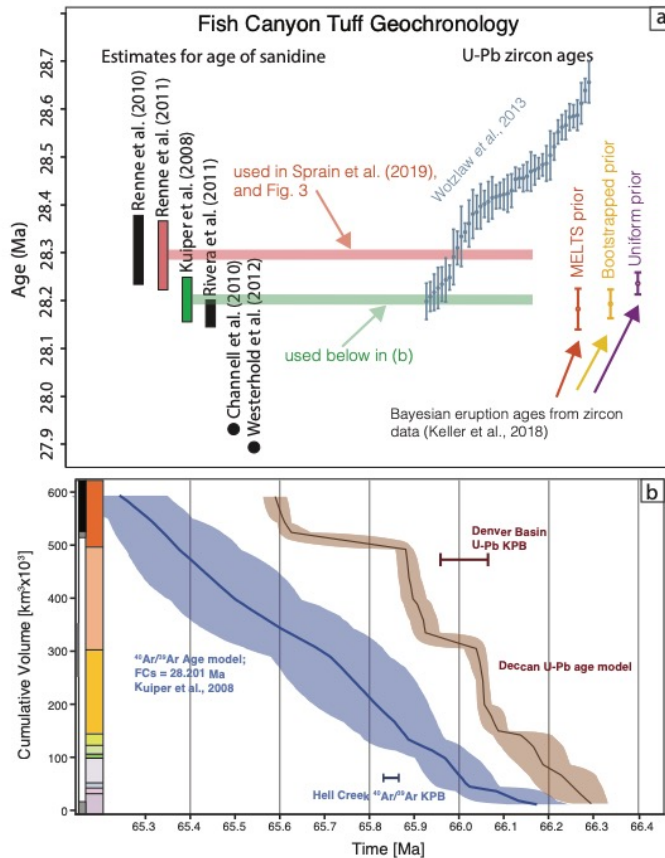


Fig. 7: Effect of choice of the age for the Fish Canyon sanidine (FCs) neutron fluence monitor on the ⁴⁰Ar/³⁹Ar dataset. (a) summary of existing estimates for the age of the FCs from the literature, generated using a variety of techniques, shown with height of bars as 2sigma uncertainties (when reported), compared to the U-Pb zircon dataset from Wotzlaw et al. (2013). Each blue dot and uncertainty bar represents a single zircon analysis from the tuff. Also shown are eruption age estimates using the Bayesian technique from Keller et al. (2018) applied to the zircon dataset. Horizontal red and green lines (with arbitrary width) are shown projected into the zircon dataset to facilitate comparison between the Renne et al. (2011) estimate for the FCs age, which was used in Sprain et al. (2019), and the widely adopted Kuiper et al. (2008) estimate. Both the Kuiper et al. (2008) and (Rivera et al., 2011) estimates agree with the U-Pb eruption estimates. (b) simplified ⁴⁰Ar/³⁹Ar and U-Pb age models from Fig. 3, but with the ⁴⁰Ar/³⁹Ar data reduced using the Kuiper et al (2008) FCs age instead of the Renne et al. (2011) FCs age. Both Deccan ages and the Chicxulub impact age shift younger by ~200 ka, and there is no overlap between the U-Pb and ⁴⁰Ar/³⁹Ar age models. The take home is that either the Deccan ⁴⁰Ar/³⁹Ar and U-Pb datasets can agree, or the FC tuff ⁴⁰Ar/³⁹Ar and U-Pb ages can agree, but not both.